16th World Conference on Earthquake, 16WCEE 2017
Santiago Chile, January 9th to 13th 2017
Paper N° 3267
Registration Code: S-R1462960954

POTENTIAL OF AMBIENT NOISE TECHNIQUES TO MONITOR INJECTION INDUCED SUBSURFACE CHANGES

A. Obermann, S. Wiemer

Swiss Seismological Service, ETH Zürich, anne.obermann@sed.ethz.ch

Abstract

One of the key challenges for the successful developement and operation of deep underground heat exchangers is to control the risk of inducing potentially hazardous seismic events. This was once again highlighted with the failures of two recent deep geothermal energy projects in Switzerland (Basel, 2006, St. Gallen, 2013).

We study tiny lapse-time changes in the coda of ambient noise cross-correlations recorded over 1 year including the different project phases. We observe a significant loss of waveform coherence of our measurements that starts with the onset of the fluid injections 4 days prior to the gas kick. We can horizontally and vertically constrain the waveform perturbation to the injection location of the fluid. We interpret the loss of coherence as a local perturbation of the medium due to the fluid injections. Using this case, we show how an ambient seismic noise analysis can be used to assess the aseismic response of the subsurface to well operations and how this method could have helped to recognize the unexpected process much earlier than the microseismic response allowed.

Keywords: ambient noise, induced seismicity, monitoring, geothermal energy

1. Introduction

In classical seismic and seismology applications, we can draw direct conclusions about the subsurface from the traveltimes of the waves. However, the Earth is more complicated than the simple layer assumption and shows heterogeneities at different scales (mountain ranges (km), fractures (m), different grains (cm-mm)). These heterogeneities cause part of the seismic waves to be multiply scattered and thus follow a longer path through the medium. These scattered waves form the late arrivals in a seismogram, also referred to as the seismic 'coda'. Despite the complex wave propagation underlying it, the waves in the coda have sampled a large volume of the medium repeatedly and are thus very sensitive to small changes in that volume. The resulting very small changes in travel time can be identified using a method called “coda wave interferometry” (CWI). Besides the detection of temporal changes in a medium, an important aspect is to know where these changes occur. With a novel inversion technique [1,2] based on 2D probabilistic sensitivity kernels [3] the horizontal location of the changes can be assessed. The depth of the changes can be estimated from a frequency analysis.

For monitoring purposes a repeated energy source is required. A powerful (and cheap) solution is offered by the omnipresent ambient seismic noise. *[4]* and *[5]* have shown that the cross-correlation function of a pair of recordings can be used to retrieve the Green’s function between two receivers, as if one of the receivers behaved like an impulsive source. After these discoveries, surface waves from ambient seismic noise cross correlations have been widely used for high-resolution imaging of the Earth’s lithosphere.

In the present paper, we demonstrate for the St. Gallen geothermal project case that recent ambient seismic noise imaging techniques provide new possibilities to monitor reservoir changes beyond the purely seismic response. The ambient seismic noise monitoring enables us to observe the aseismic response of the reservoir to operator activities that remained undetected with the standard monitoring of microseismicity. We observe a significant loss of waveform coherence parallel to the injection tests and prior to the M_L3.5 event that is linked to a medium change and not an artifact of microseismicity or local source changes. We estimate the spatial distribution of the change horizontally with an inversion procedure and vertically with help of a spectral analysis. The results show that the spatial distribution of the changes corresponds well with the injection location.

2. Methods

2.1. Ambient noise cross correlations

In seismology, [4] were the first to show the emergence of surface waves from cross-correlations of earthquake coda waves (Fig. 1 for a schematic view). One year later, [5] used ambient seismic noise for the Green’s function reconstruction, opening the way to numerous applications in seismology.

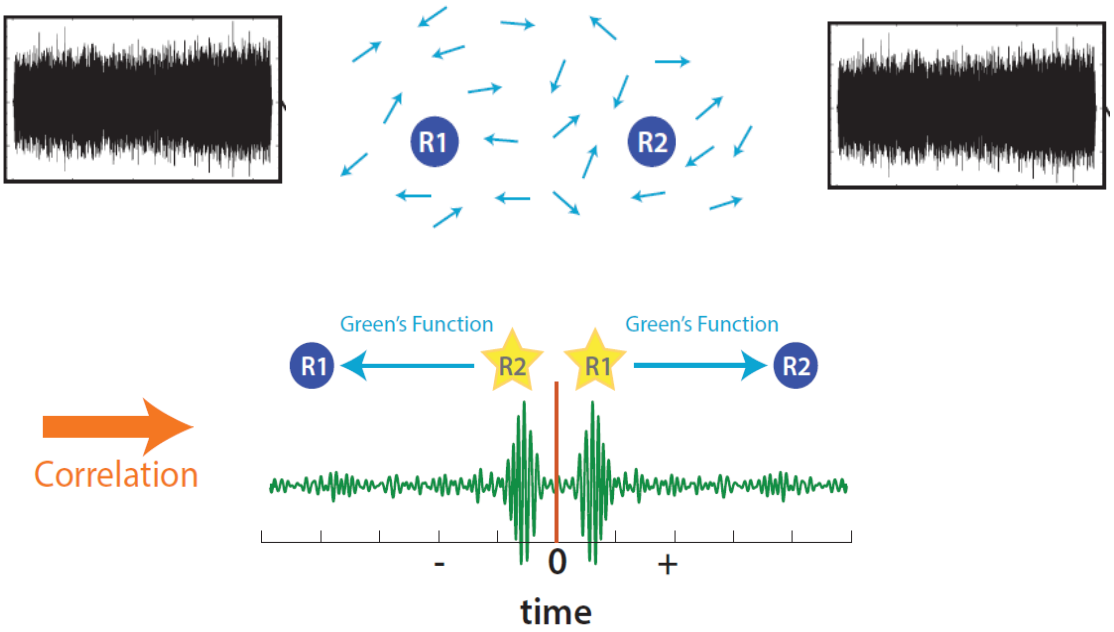

Figure 1: Schematic representation of the process of ambient noise cross-correlation (Courtesy of Pierre Boué)

2.2. Coda wave interferometry

In a regime where multiple scattering is strong, waves traveling from a source to a receiver can follow many trajectories and no direct conclusions about the subsurface can be drawn anymore from the traveltimes of the waves (Fig. 2). These multiply scattered waves are called coda waves.

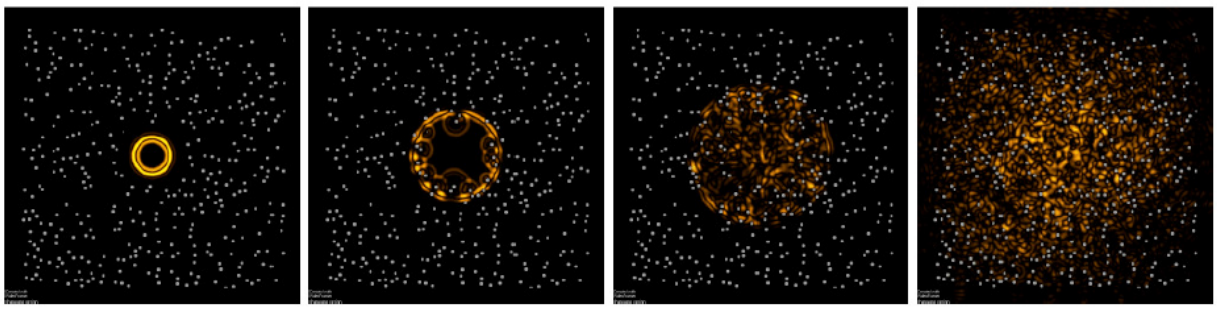

Figure 2: Snapshots at increasing times of a wave propagating in a numerical simulation of a heterogeneous medium. At initial times (left) there are no scatterers and the direct waves can be observed. At later times, the waves encountered the medium heterogeneities and the wave propagation becomes very complex (Figure from *[6]*).

Besides their random character, coda waves are highly repeatable, such that if the medium remains unchanged over time, subsequent measurements of coda waveforms would be identical. Additionally, coda waves sample the medium very densely and become sensitive to even tiny perturbations of its mechanical (velocity, pressure, etc) or structural (change of scatterer position, for instance due to fracturing) properties. This feature makes them ideal for monitoring purposes and has led to the development of the coda-wave interferometry (CWI) technique [7,8] Since then, the detection of temporal changes with coda waves has been successfully applied in different areas in seismology.

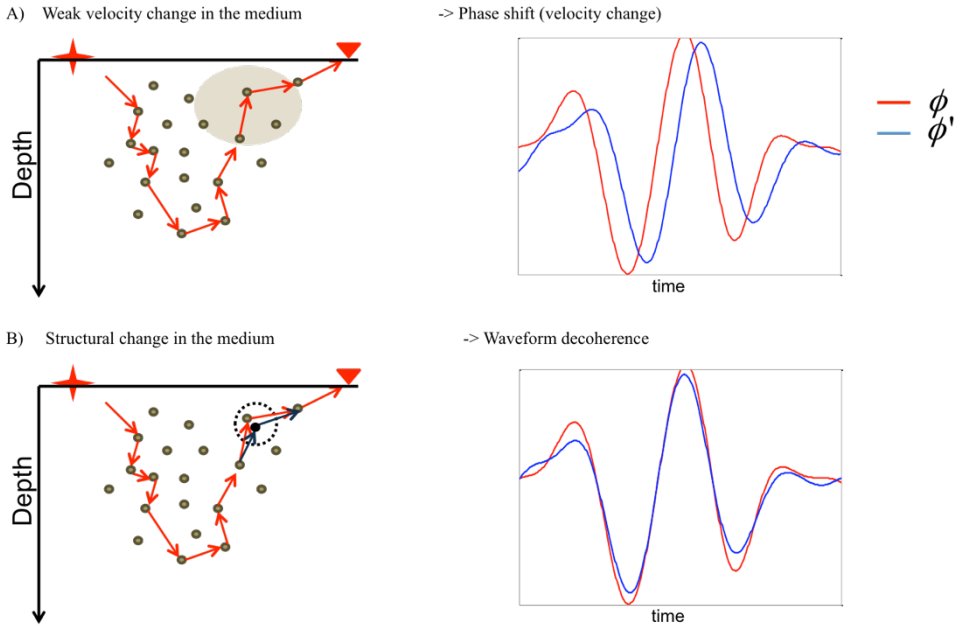

Figure 3: Schematic representation of the effect of a (A) weak velocity change and a (B) structural change in the medium on the wave Φ'(blue) compared to a wave Φ (red) that has not encountered the change. The weak velocity change causes a phase shift. The structural change causes waveform decoherence.

We can imagine two different types of changes in the diffuse coda (Fig.3). A weak velocity/pressure change in the medium would result in a phase shift (apparent velocity change) of the passing waves compared to waves passing prior to the change. A modification of the scattering properties of the medium (structural change), would result in a change of the waveform and consequently, a loss of waveform coherence. We can quantify both types of changes with the stretching technique [9].

2.2. Locating medium changes using probabilistic sensitivity kernels

Beside the detection of the temporal changes, an important aspect is the localization of the changes. Using the diffuse character of coda waves, *[1,2]* developed an imaging procedure that allows the spatial localization of these medium changes on the horizontal plane (2D). This localization method makes use of a 2D probabilistic sensitivity kernel (Fig. 4) that is based on the assumption that coda waves are dominated by surface waves. As a consequence, the localization of the medium changes can only be done on the horizontal plane.

The method has been successfully applied to forecast the location of upcoming volcanic eruptions at Piton de la Fournaise volcano, La Réunion Island [10]; study the mechanical weakening of the crust after the 2008 M7.9 Wenchuan, China, earthquake [11]; study the extension of the injection induced changes in geothermal settings in Switzerland [12,13]; as well as in numerical simulations [14,15].

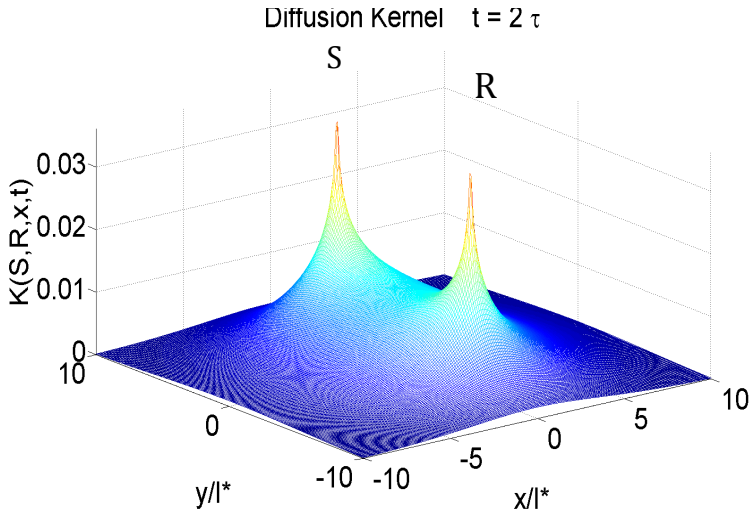

Figure 4: Spatial representation of the sensitivity kernel that describes the statistical time the waves spent in each part of the medium. The two peaks (R, S) indicate the position of the station pair. The time statistically spent in a region decreases with its distance to the stations (Figure from [10]).

3. Application to the St. Gallen (Switzerland) geothermal project * a more detailed version of this section is published in [12]

3.1. The St. Gallen Project

The deep geothermal project in the vicinity of the city of St. Gallen, Switzerland, targeted a hydrothermal resource at a depth of 3.5 -5 km. The project was considered to be of low seismic risk, as hydraulic stimulation would only be needed if flow rates >50 L/s were not found. The project's target was the Mesozoic Malm and Muschelkalk layers of the Molasse sedimentary basin, which have already been successfully exploited in several deep geothermal projects in Southern Germany. To improve the chances of finding high permeabilities, preexisting fault zones were targeted.

In the first half of 2013 an injection well was drilled to a depth of 4500 m. To gain a better understanding of the reservoir, a small-scale injectivity test was performed on 14 July 2013. During the test, only 12 micro-earthquakes with a maximum magnitude of M_L0.1 were detected. On 17 July, two acid stimulations were performed, The seismicity (roughly 40 events) associated with these tests did not exceed magnitude M_L 0.2 and was judged to be well within the expected range. On 19 July gas (90% methane) unexpectedly entered the borehole from an unknown source at depth. Operators decided to take measures to fight the gas kick and secure the well. Large amounts of drilling mud were pumped into the well to push the gas back into the formation, successfully leading to a steady decrease of the pressure at the well head. This well control procedure was accompanied by an intensifying sequence of induced earthquakes. On 20 July, the largest event of the sequence occurred, with a magnitude of M_L 3.5 (M_w 3.3).

While the microseismicity at St. Gallen could be monitored down to levels of M_L– 1.1 [16] it only provided information on the seismic response of the underground. Yet aseismic responses to the injections that might give us important insights to the processes involved in deep-underground injections could not be resolved with standard seismic analysis.

3.2. The seismic network

The seismic network (Fig. 5B) consisted of five broadband stations, one 4.5 Hz borehole sensor, and three short-period sensors. The short black line in Fig. 5B marks the horizontally projected position of the injection well. The broadband stations and the borehole sensor recorded data from August 2012 until at least the end of 2013, while the short-period stations started recording only prior to the injection tests in July 2013.

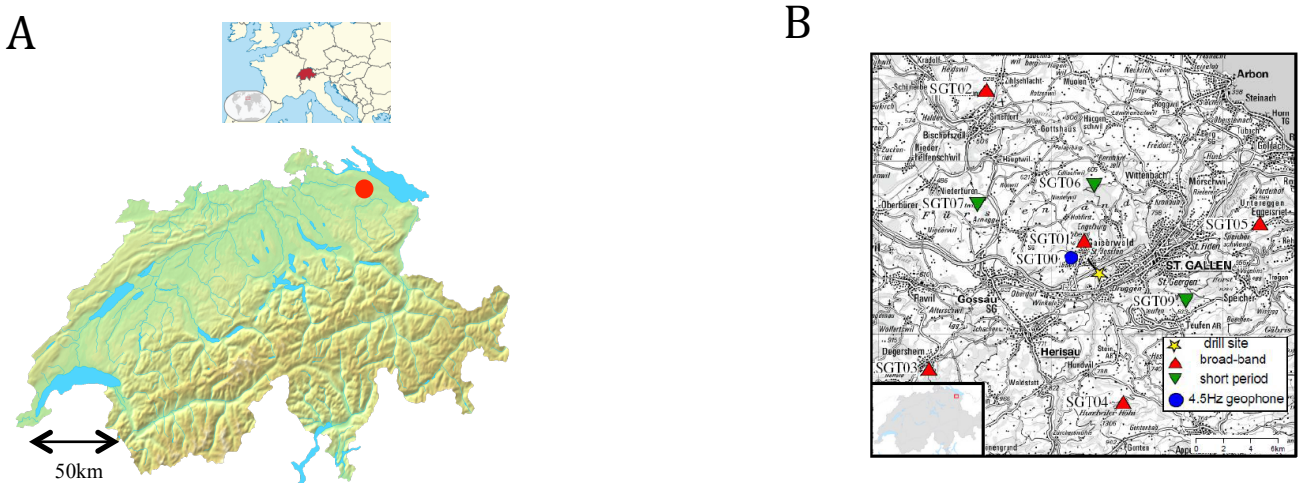

Figure 5: A) The St. Gallen geothermal site in the Molasse Basin in the NorthEast of Switzerland.) Seismic stations used in this study: five 120 s broadband stations (SGT01–SGT05), one 4.5 Hz borehole geophone (SGT00) and three 1 Hz short-period sensors (SGT06, SGT07, and SGT09).

3.3. Ambient noise cross correlation

We analyze the vertical component of the continuous noise records and apply preprocessing steps similar to *[17,18]* prior to the calculation of the cross correlations. We work with 0.1-1Hz spectrally whitened data. An example of the computed cross-correlation functions after processing is shown for two exemplary station pairs in Fig. 6. These station pairs are relatively noisy but a coherent signal can still be seen until about 50 s in the coda.

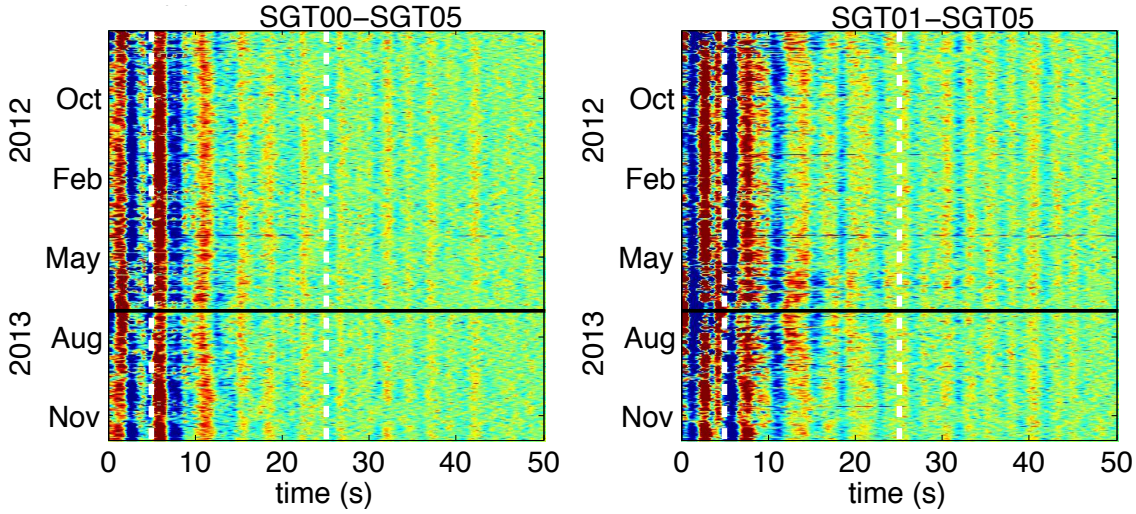

Figure 6: Symmetrized cross-correlation function for two exemplary station pairs. The horizontal black line marks the M_L3.5 event. The vertical white dashed lines mark the time window used for the stretching (Figure from [12]).

3.4. Temporal variations in the coda

To quantify the temporal variations in the coda of the correlations, we use the stretching technique [9]. We compare, for each receiver pair a 5 day long stack around day *d* to a reference stack that is the average over all available daily cross-correlation functions.

In Fig.7 we have a closer look at the loss of coherence during the period of injection activity in July 2013 (beginning of July to the end of August 2013). We study two different subsets of exemplary station pairs. In Fig.7a we study station pairs with trajectories that cross the injection area (as indicated in the map on the left of Fig. 7a), while in Figure 7b we study station pairs with trajectories that do not cross the injection area (as indicated in the map on the left of Figure 7b). The solid gray lines mark the injection test and the acid treatments. The light gray line indicates the earliest possible influence of the injection on the displayed data due to the 5 days stack used in the stretching procedure. The yellow line marks the gas kick, and the solid red line the M_L3.5 earthquake on 20 July. The thin red line marks the end of the influence of the earthquake on the displayed data due to the 5 days stack. The station pairs at a distance from the stimulation tests (Fig. 7b) do not show a significant loss of coherence in July 2013, whereas we notice a clear loss of coherence for all displayed station pairs that are in the vicinity of the injections (Fig. 7a). The coherence loss is strongest on 19 and 20 July 2013 with the gas kick and the M_L3.5 earthquake. For all displayed station pairs we notice clearly that the distortion of the waveform starts with the onset of the influence of the first injection (14 July), prior to the earthquake.

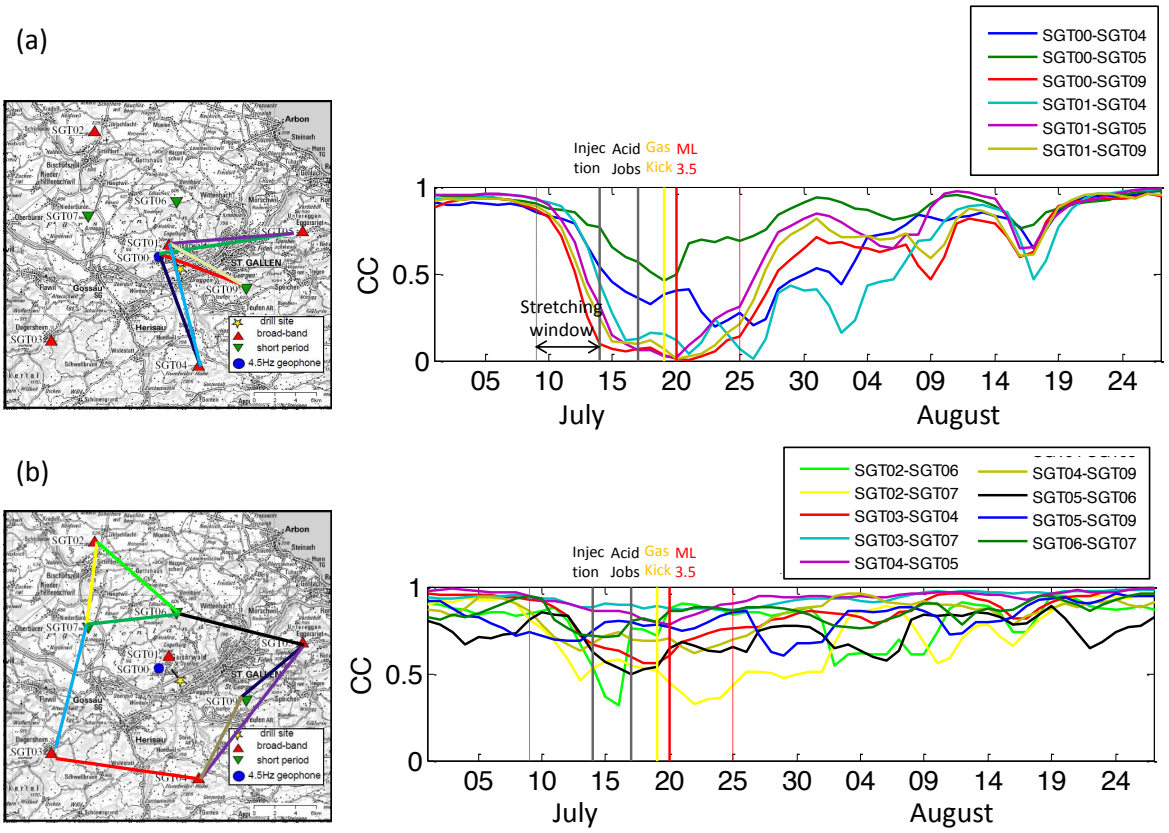

Figure 7: Observed waveform coherence (*CC*) for the indicated station pairs: (a) close to the injections and (b) further away from the injections. The vertical lines in the *CC* plots mark the injection tests, the gas kick and the M_L3.5 earthquake (Figure from [12]).

3.5. Locating medium changes

We invert the changes that occurred, averaged over the month of July relative to the rest of the observation period (2012 – 2013). The result is displayed in Fig. 8 as a map of the scattering cross-section density σ that is associated with the strength and size of the medium change. The changes that we observe are spatially constrained within 3–6 km of the injection well suggesting that they are related to the injection activities. The maximum of the changes is northwest of the injection well, which might be slightly biased by the network setup.

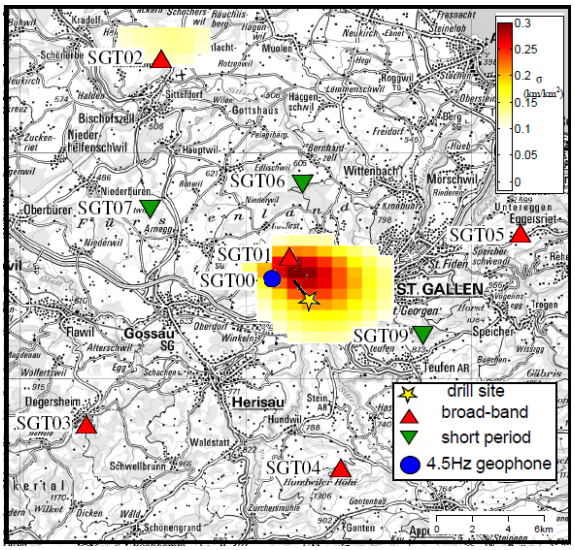

Figure 8: Scattering cross-section density changes derived by least squares inversion averaged over July 2013. The observed changes are around the injection well, indicating a causal relationship with the activities at the well (Figure from [12]).

4. Interpretation and conclusion

We observe a significant loss of waveform coherence in the seismic coda that starts with the injection of small amounts of water and acid into the well. The loss of coherence reaches its maximum (with a total loss of coherence observed at some station pairs) at the time of the gas kick or the M_L3.5 earthquake, depending on the region sampled by the station pairs. Roughly 30 days after the M_L3.5 event, the coherence on all station couples recovers to the initial values. We are certain that the loss of coherence is due to a perturbation in the subsurface. We can spatially constrain this perturbation within a few kilometers around the injection interval, both horizontally and vertically (not shown here, please see [12]).

To explain the waveform decoherence, we speculate about three possible scenarios:

1. *Changes in attenuation and/or reflectivity due to the gas*. Methane gas hydrate can have a dramatic effect on seismic wave attenuation [*19*] and reflectivity [*20*]. Shallow gas accumulations are recognized as strong reflection amplitude anomalies due to the large acoustic impedance contrast between gas-filled and sand-silt-filled media. This could explain the strength of the decoherence as well as its return to the initial values once the gas is back to its original formation and the possibly remaining gas concentration dispersed.

2. *Critically prestressed fault*. The drilling targeted a fracture zone that extends several kilometers to the North and South and has a width of possibly 100 m. As indicated by [21] this fault zone is optimally oriented in the present-day stress field. The fault was therefore most likely critically prestressed and even small pore pressure increases could initiate local slip on fault patches. These pore pressure changes may then have caused

perturbations of the seismic waveforms.

3. *Pore pressure changes due to injected water or released gas*. Pore pressure changes could be induced either by the injected water volume or by the released gas. Since the 1950s hydrocarbon exploration has been conducted in the Alpine foreland [*22*]. The gas often occurs in highly overpressured pockets, rendering hydrocarbon exploration in the Alpine thrust belt a special challenge as pore pressure may be very close to fracturing pressure [*22*]. From this experience, gas in St. Gallen was mainly expected in much shallower formations than the targeted Mesozoic Malm and Muschelkalk layers. It is possible that the pore pressure change induced by the injections interacted with the overpressured PCT, resulting in a significant stress change that acted on the numerous faults and fault patches within the fracture zone and caused a significant, locally constrained, perturbation of the seismic waveforms.

In conclusion, it was likely a combination of the described effects that caused the remarkable loss of coherence that we observe during the injection period in St. Gallen.

We are convinced that ambient noise correlations offer interesting possibilities to assist the monitoring of engineering projects involving subsurface stimulations. Particularly when applied to denser networks, ambient noise monitoring techniques could also help to better understand reservoir dynamics and mitigate associated risks.

5. Acknowledgements

We would like to thank the Sankt Galler Stadtwerke for access to data and information. The research leading to these results has received funding from the European Community's Seventh Framework Programme under grant agreement 608553 (Project IMAGE) and the Swiss Federal office of Energy with the project GEOBEST. To request seismological waveform data used in this study, please contact the Swiss Seismological Service.

6. References

[1] Larose, E., T. Planès, V. Rossetto, and L. Margerin (2010), Locating a small change in a multiple scattering environment, *Appl. Phys. Lett.*, *96*, 1–3.

[2] Rossetto, V., Margerin, L., Planès, T., and Larose, E. (2011). Locating a weak change using diffuse waves: Theoretical approach and inversion procedure. *J. Appl. Phys.*, 109(034903): 1–11.

[3] Pacheco, C., and R. Snieder (2005), Time-lapse travel time change of multiply scattered acoustic waves, *J. Acoust. Soc. Am.*, *118*, 1300–1310.

[4] Campillo, M., and A. Paul (2003), Long-range correlations in the diffuse seismic coda, *Science*, *299*, 547–549.

[5] Shapiro, N. M., and M. Campillo (2004), Emergence of broadband Rayleigh waves from the correlations of the ambient seismic noise, *Geophys. Res. Lett.*, *31*, L07614, doi:10.1029/2004GL019491.

[6] Paul, A., Campillo, M., Margerin, L., Larose, E., and Derode, A. (2005). Empirical synthesis of time-asymmetrical green functions from the correlation of coda waves. *Journal of Geophysical research*, 110(B8):B08302.

[7] Poupinet, G., Ellsworth, W.L.., and Frechet, J. (1984). Monitoring velocity variations in the crust using earthquake doublets: an application to the Calaveras fault, California. *J. Geophys. Res.*, 89(B7):5719–5731.

[8] Snieder, R. (2006), The theory of coda wave interferometry, *Pure Appl. Geophys.*, *163*, 455–473.

[9] Sens-Schönfelder, C. and Wegler, U. (2006). Passive image interferometry and seasonal variations of seismic velocities at Merapi Volcano, Indonesia. *Geophys. Res. Lett.*, 33(21):L21302.

[10] Obermann, A., T. Planès, E. Larose, and M. Campillo (2013a), Imaging preeruptive and coeruptive structural and mechanical changes of a volcano with ambient seismic noise, *J. Geophys. Res. Solid Earth*, *118*, 6285–6294, doi:10.1002/2013JB010399.

[11] Obermann, A., B. Froment, M. Campillo, E. Larose, T. Planès, B. Valette, J. H. Chen, and Q. Y. Liu (2014a), Seismic noise correlations to image structural and mechanical changes associated with the Mw 7.9 2008 Wenchuan earthquake, *J. Geophys. Res.*, *119*, 3155–3168, doi:10.1002/2013JB010932.

[12] Obermann, A., T. Kraft, E. Larose, and S. Wiemer (2015), Potential of ambient seismic noise techniques to monitor the St. Gallen geothermal site (Switzerland), *J. Geophys. Res. Solid Earth*, *120*, doi:10.1002/2014JB011817.

[13] Hillers, G., S. Husen, A. Obermann, T. Planès, M. Campillo, and E. Larose (2015), Noise based monitoring and imaging of aseismic transient deformation induced by the 2006 Basel reservoir stimulation, *Geophysics*, doi:10.1190/GEO2014-0455.1.

[14] Planès, T., E. Larose, L. Margerin, V. Rossetto, and C. Sens-Schönfelder (2014), Decorrelation and phase-shift of coda waves induced by local changes: Multiple scattering approach and numerical validation, *Waves Random Complex Medium*, *2*, 1–27.

[15] Planès, T., E. Larose, V. Rossetto, and L. Margerin (2015), Imaging multiple local changes in heterogeneous media with diffuse waves, J. Acoust. Soc. Am., 137(2), 660–667.

[16] Edwards, B., T. Kraft, C. Cauzzi, P. Kästli, and S. Wiemer (2015), Seismic monitoring and analysis of a deep geothermal project in St. Gallen, Switzerland, *Geophys. J. Int.*, *201*, 1022–1039.

[17] Sabra, K. G., P. Gerstoft, P. Roux, W. A. Kuperman, and M. Fehler (2005), Extracting time-domain Green's function estimates from ambient seismic noise, *Geophys. Res. Lett.*, *32*, L03310, doi:10.1029/2004GL021862.

[18] Bensen, G. D., M. H. Ritzwoller, M. P. Barmin, A. L. Levshin, F. Lin, M. P. Moschetti, N. M. Shapiro, and Y. Yang (2007), Pre-eruptive migration of earthquakes at the Piton de la Fournaise volcano (Réunion Island), *Geophys. J. Int.*, *169*, 1239–1260.

[19] Priest, J. A., A. I. Best, and C. R. Clayton (2006), Attenuation of seismic waves in methane gas hydrate-bearing sand, *Geophys. J. Int.*, *164*,149 – 159.

[20] Ghazali, A. R. (2011), True-amplitude seismic imaging beneath gas clouds, TU Delft, Delft, Netherlands.

[21] Heuberger, S., and H. Naef (2012), The St. Gallen Fault Zone (NE Switzerland): A long-lived, multiphase structure in the North Alpine Foreland—Insights from high-resolution 3D seismic data. paper presented at 10th Swiss Geoscience Meeting, 2. Structural Geology, Tectonics and Geodynamics.

[22] Huber, K., O. Lettau, H. Meinschien, M. Müller, F. Nieberding, and K. Weggen (1990), Gas exploration beneath the Bavarian Alps—A technical challenge, in *Super-Deep Continental Drilling and Deep Geophysical Sounding*, edited by K. Fuchs et al., pp. 191–202, Springer, Berlin.